Unsupervised Probabilistic Model Averaging Across Nested Transport Models for Brain Permeability Mapping at 0.55 Tesla

Hassan Bagher-Ebadian, PhD[1,2], Joshua P. Kim, PhD[1,2], Eric A. Mellon, MD, PhD[1,2], Stephen L. Brown, PhD[1,2], Lisa R. Rogers, MD[1], James R. Ewing, PhD[1,2], Benjamin Movsas, MD[1,2] and Kundan S Thind, PhD[1,2]

[1]Henry Ford Health, Detroit, MI, [2]Michigan State University, East Lansing, MI

2026 JULY 19–22 VANCOUVER, BC
JOINT AAPM | COMP MEETING

ABSTRACT

Purpose: To develop and evaluate an unsupervised probabilistic nested model selection (PNMS) framework for quantitative brain permeability mapping using 0.55T DCE-MRI.

Methods: Four patients with brain metastases underwent whole-brain DCE-MRI on a Siemens MAGNETOM Free.Max 0.55T system. A Kohonen self-organizing map was trained using 292,630 measured and simulated ΔR_1 profiles and compared with deterministic nested model selection (NMS).

Results: PNMS showed strong agreement with deterministic NMS in leaky tumor regions (DSC=0.782 for Model-2 and 0.873 for Model-3) while reducing noise sensitivity and producing spatially coherent probability maps that captured voxel-wise heterogeneity and model uncertainty.

Conclusion: PNMS enables robust and physiologically meaningful permeability mapping at 0.55T, supporting quantitative DCE-MRI on modern low-field MRI systems.

Session: Therapy.
PBN: SU-315-GPD-T-253
Abstract ID: 24751

CONTACT

Hassan Bagher-Ebadian, PhD

Professor, Department of Radiation Oncology
Henry Ford Health
2799 West Grand Blvd.
Detroit, MI 48202, USA
Email: hbagher1@hfhs.org

Professor, Department of Radiology
College of Human Medicine
Michigan State University
846 Service Rd.
East Lansing, MI 48824, USA

Professor, Clinical Faculty
College of Osteopathic Medicine (MSUCOM)
Michigan State University
846 Service Rd.
East Lansing, MI 48824, USA
Email: baghere1@msu.edu

Adjunct Professor, Department of Physics
Oakland University
Rochester, MI 48309, USA

Phone: +1 (313) 648-5660

INTRODUCTION

- Dynamic contrast-enhanced (DCE)-MRI provides quantitative assessment of microvascular permeability, but low-field imaging (0.55T) suffers from reduced SNR and uncertainty in voxel-wise pharmacokinetic model selection.
- Conventional nested model selection (NMS) employs hard winner-take-all decisions that can be sensitive to noise and fail to capture mixed or transitional transport behavior commonly observed in heterogeneous tumors.
- We propose an unsupervised probabilistic nested model selection (PNMS) framework based on Kohonen self-organizing maps that performs voxel-wise probabilistic model averaging, enabling uncertainty-aware and robust permeability mapping on the Siemens MAGNETOM Free.Max 0.55T system.

METHODS AND MATERIALS

- Four untreated patients with brain metastases (IRB# 15622-01) underwent whole-brain DCE-MRI on a Siemens MAGNETOM Free.Max 0.55T system using a sequence-optimized protocol for low-field imaging.
- Baseline T_1 maps were obtained using dual-flip-angle VIBE (2°/15°), followed by TWIST DCE acquisition (TR/TE/FA = 4.48/2.02 ms/15°) with 7.04 sec temporal resolution and whole-brain coverage.
- Signal intensity curves were converted to longitudinal relaxation-rate changes (ΔR_1), and voxel-wise deterministic nested model selection (NMS) was performed using three physiologically nested transport models representing normal vasculature, unidirectional leakage, and bidirectional exchange (see Figure 1).
- Pharmacokinetic parameters (v_p, K^{trans}, and k_{ep}) were estimated for each model, and ±30% parameter perturbations were analytically simulated to increase variability and generate additional analytical ΔR_1 profiles.
- A total of 292,630 normalized measured and simulated ΔR_1 profiles with corresponding NMS labels were used to train an 8×8 Kohonen self-organizing map (K-SOM).
- K-SOM-based probabilistic nested model selection (PNMS) was implemented using a 50% probability threshold and compared with deterministic NMS using Dice similarity coefficients (DSC).

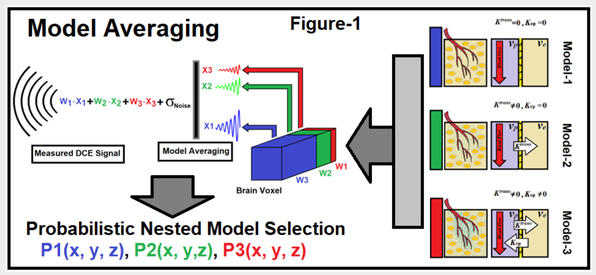

RESULTS

- Subfigures A-D show the 8×8 K-SOM feature spaces, demonstrating clear and interpretable separation of the three physiologically nested transport models and preservation of their spatial organization in the fused representation.
- Subfigures E-G present the corresponding iso-contour maps, revealing compact probability regions with high model confidence and smooth transitions between competing models, reflecting graded uncertainty rather than abrupt boundaries.
- Subfigure H displays the ΔR_1 map at 6.08 min, highlighting distinct signal dynamics associated with normal vasculature, unidirectional leakage, and bidirectional exchange.
- Subfigures I-J compare the deterministic NMS and probabilistic PNMS maps for Models 1, 2, and 3. The results demonstrate strong spatial agreement between the two approaches, particularly for Model 2 (DSC = 0.782 [0.739–0.825]) and Model 3 (DSC = 0.873 [0.837–0.909]), while PNMS provides smoother, more spatially coherent probability distributions.
- Subfigures K-L present an additional example comparing NMS and PNMS maps. PNMS shows excellent agreement with deterministic NMS while identifying voxels with mixed or transitional transport behavior, capturing model uncertainty and tissue heterogeneity.

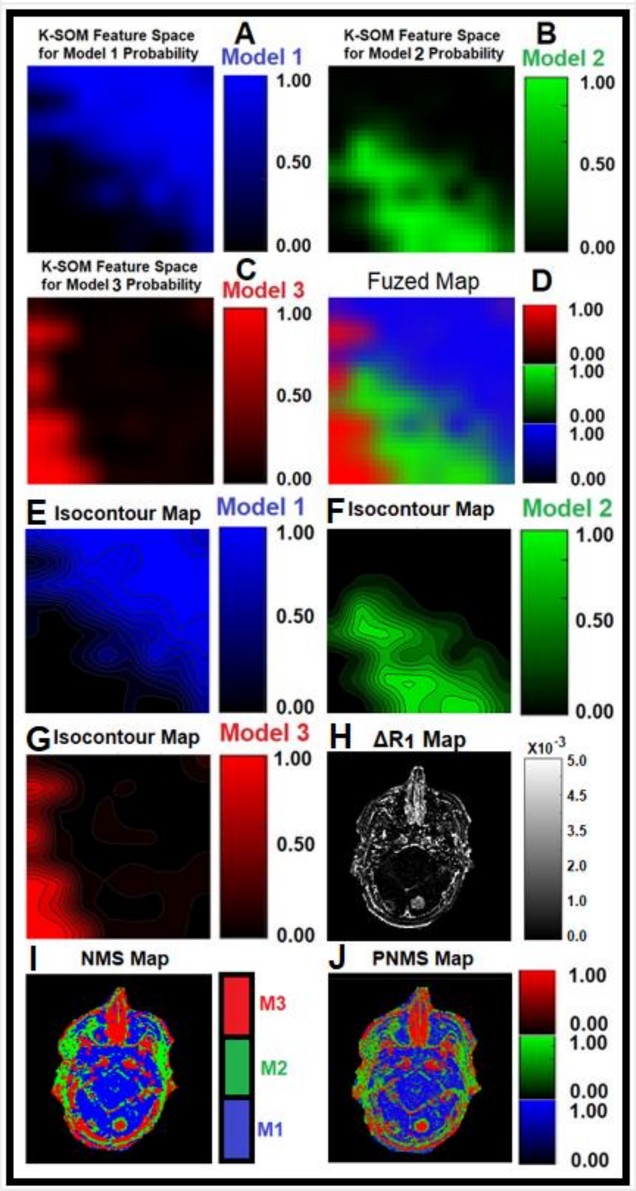

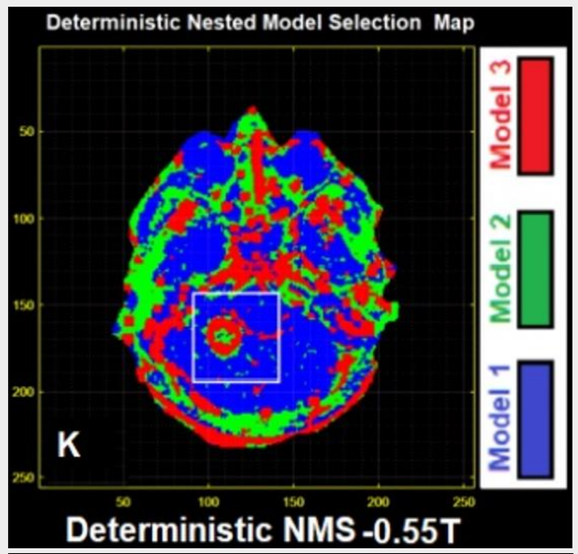

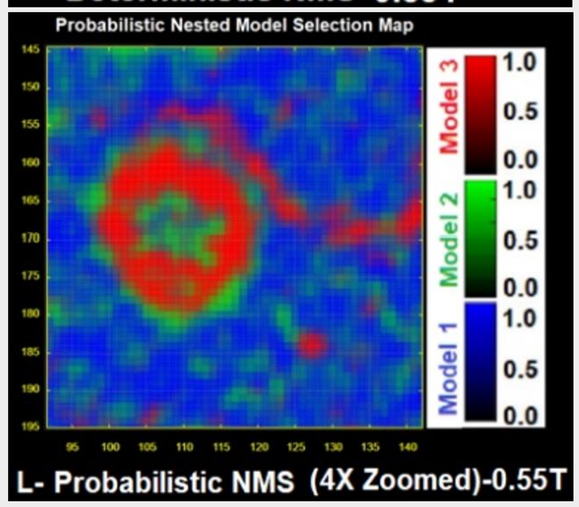

DISCUSSION

- PNMS replaces hard winner-take-all model selection with probabilistic weighting, improving robustness to noise and arterial input dispersion, which are amplified at 0.55T.
- By explicitly representing model uncertainty and transitional transport states, PNMS produces more spatially coherent and physiologically meaningful permeability maps than deterministic NMS.
- These findings support uncertainty-aware quantitative DCE-MRI and provide a scalable pathway for extending advanced permeability imaging to clinically accessible low-field MRI systems.

CONCLUSIONS

PNMS enables robust, uncertainty-aware brain permeability mapping at 0.55T. Probabilistic model averaging improves the stability and spatial coherence of DCE-MRI biomarkers. This framework supports quantitative DCE-MRI on clinically accessible low-field MRI systems.

REFERENCES

[1] Bagher-Ebadian H, et al. MRM. 2012;68:241–251.

[2] Ewing JR, Bagher-Ebadian H. NMR Biomed. 2013;26:1028–1041.

[3] Bagher-Ebadian H, et al. Sci Rep. 2025;15:1786.